SCIENCE CHINA
Physics, Mechanics & Astronomy

• Article •

May 2013 Vol.56 No.5: 910–915
doi: 10.1007/s11433-013-5024-6

A VHF band HTS filter based on modified single-spiral resonators for radio astronomy application

LI Chao, SUN Liang, WANG Jia, BIAN YongBo, YU Tao, LI Fei, LI ChunGuang, LI Hong, GU ChangZhi & HE YuSheng*

Institute of Physics, Chinese Academy of Sciences, Beijing 100190, China

Received January 17, 2012; accepted March 31, 2012; published online February 22, 2013

A 10-pole quasi-elliptic bandpass filter (BPF) with a relatively wide passband in the very high frequency (VHF) band was designed and fabricated using YBCO thin films deposited on both sides of a $LaAlO_3$ substrate. Single-spiral resonators were modified to generate strong coupling and reduce the parasitic coupling. We analysed the coupling polarities between the modified resonators. Two pairs of attenuation poles were introduced in the filter for sharp cut-off response. The measurements showed that the filter has a centre frequency of 255.8 MHz, fractional bandwidth of about 12.3%, insertion loss of smaller than 0.265 dB, and the return loss in the passband of better than 17.5 dB, in good agreement with computer simulations.

HTS filter, spiral resonator, fractional bandwidth, coupling polarity, parasitic coupling

PACS number(s): 85.25.Am, 74.78.Bz, 84.30.Vn

Citation: Li C, Sun L, Wang J, et al. A VHF band HTS filter based on modified single-spiral resonators for radio astronomy application. Sci China-Phys Mech Astron, 2013, 56: 910–915, doi: 10.1007/s11433-013-5024-6

Radio astronomy observation is one of the major beneficiaries of high-temperature superconductivity (HTS) microwave application [1–3]. Compared with other systems with HTS microwave devices, the radio astronomy telescope receivers introduce no extra burden of cooling devices. Recently, National Astronomical Observatories (NAO), Chinese Academy of Sciences, Beijing, China, plans to use HTS filters to observe pulsars in the very high frequency (VHF) band. The HTS filter provides extremely high selectivity and high out-of-band rejection. Therefore it can remarkably improve the sensitivity of the receivers and reduce the out-of-band interference such as television, radio broadcast, and communication signals.

HTS microstrip filters are fabricated with superconducting thin films deposited on a 2 or 3 inch wafer. The resonance frequency of the resonator is inversely proportional to the physical length of the half wavelength. Filters with lower centre frequency take up larger film areas. Most of the HTS microstrip filters work in the upper ultrahigh frequency (UHF) or gigahertz (GHz) frequencies because of the limitation of the wafer size [4–7]. It is difficult to fabricate a filter working in VHF band on a 2 inch wafer. For reducing the size of the filters, many novel and compact resonators have been proposed [8–11]. However, compact structure is contradictory to strong coupling between resonators because compact resonators usually have weak field radiation. On the other hand, strong field radiation always results in strong parasitic coupling. Most of the reported HTS filters in VHF band have narrow passbands. In this paper, we report the design and fabrication of a HTS microstrip filter with a relatively wide passband in VHF band using modified single-spiral resonators. Compared to conventional single-spiral resonators, the modified resonators exhibit stronger direct coupling strength, relatively weak parasitic coupling, and larger flexibility to adjust input and output admittances, satisfying all requirements for our filter in

*Corresponding author (email: yshe@aphy.iphy.ac.cn)

VHF band.

1 Resonator design

Figure 1 shows four types of resonators with compact structure, all desirable for miniaturized filters: (i) single-spiral (Figure 1(a)), (ii) dual-spiral (Figure 1(b)), (iii) spiral-in-spiral-out (Figure 1(c)), and (iv) quasi-lumped element resonators (Figure 1(d)). The four resonators are all suitable for constructing filters at a low frequency such as VHF. The coupling strength between the same type of resonators is studied through a full-wave electromagnetic (EM) simulation [12]. With the same resonant frequency (255 MHz) and gap between resonators (0.2 mm), the sequence of the coupling strength can be determined: (i)>(ii)>(iii)>(iv). By changing the gap and the direction of the spirals, the sequence of resonators (ii) and (iii) can be reversed, while the single-spiral structure (i) always exhibits the strongest coupling. Wider bandwidth filters are required for radio astronomy applications, and the specific requirement of the fractional bandwidth in the present work is targeted at 12%. Therefore, the single-spiral resonator was chosen to design our wideband filter in VHF band due to its compact structure and relatively strong field radiation. However, the coupling strength between conventional single-spiral resonators is still not high enough. The required largest magnitude of the coupling coefficient in the present study is approximately 0.115. When two conventional single-spiral resonators with 0.1 mm in linewidth and interspace are separated by a gap of 0.1 mm, the coupling coefficient is less than 0.086 at 255 MHz. It is necessary to enhance the coupling strength between resonators.

The coupling coefficient k of resonators is defined as the ratio of coupled energy to stored energy [13],

$$k = \frac{\iiint \varepsilon E_1 \cdot E_2 \mathrm{d}v}{\sqrt{\iiint \varepsilon |E_1|^2 \mathrm{d}v + \iiint \varepsilon |E_2|^2 \mathrm{d}v}} + \frac{\iiint \mu H_1 \cdot H_2 \mathrm{d}v}{\sqrt{\iiint \mu |H_1|^2 \mathrm{d}v + \iiint \mu |H_2|^2 \mathrm{d}v}}, \quad (1)$$

where E and H represent the electric and magnetic field vectors, respectively, and the volume integrals are taken over all effected regions with permittivity of ε and permeability of μ. From eq. (1), we see that k includes electric and magnetic contributions. For the typical single-spiral resonators, with one end of the microstrip on the edge and the other at the center, there are two types of couplings [1]. If the two coupled spiral resonators are wound in the same direction (Figure 2(a)), electronic and magnetic couplings are of the same sign. The absolute value of k is equal to the sum of absolute values of the two contributions. If the two spiral resonators are wound in the opposite directions (Figure 2(b)), electric and magnetic couplings are of opposite signs, partially cancelling each other. Therefore the sign of k is determined by the stronger coupling and its magnitude is smaller than that in the previous case. Full-wave EM simulation software Sonnet was used to obtain accurate coupling coefficients. In the simulations, the 0.5 mm $LaAlO_3$ substrate has a relative dielectric constant of ε_r=23.75. Relative polarity (+ or −) of coupling coefficient could be determined by the phase of S_{21}. We come to the following conclusions from extensive simulations: (i) the coupling between resonators winding in the same spiral direction (Figure 2(a)) always has the same sign in relative polarity, which can be defined as negative; (ii) the coupling between resonators winding in the opposite spiral directions (Figure 2(b)) has two polarities, which we define as negative when electric coupling is larger than magnetic coupling and vice versa.

For enhancing the electric coupling, parallel finger structure is added to the single-spiral resonator as shown in Figure 3(a). Another way is to widen the outside end (Figure 3(b)) because a wider outside end can accumulate more charges to generate stronger electric field [1]. We compare the coupling strength of the two kinds of resonators in Figures 3(a) and (b). Simulations demonstrate that the resonators with parallel finger exhibit stronger coupling than the ones with wide outside end (Figure 3(c)). A qualitative explanation follows the simulations. Parallel fingers increase the overlap region of electric fields of the coupled resonators, leading to a larger volume integral in eq. (1). Another benefit by the parallel fingers is to reduce the parasitic coupling. As shown in Figure 3(d), two resonators with a large separation could generate strong coupling by the parallel fingers, while their main bodies have very weak coupling. In our simulations in sect. 2, we will show that this method

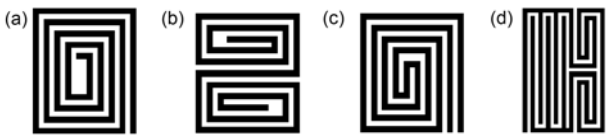

Figure 1 Four types of resonators with the compact structure: (a) single-spiral, (b) dual-spiral, (c) spiral-in-spiral-out, and (d) quasi-lumped element resonators.

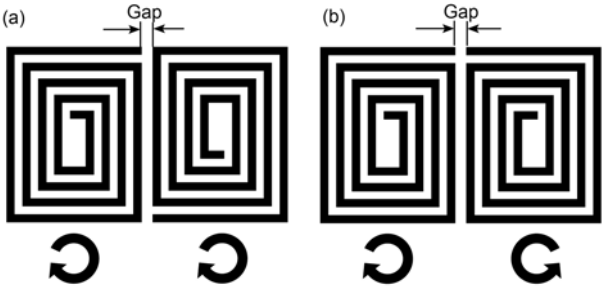

Figure 2 Coupled single-spiral resonators winding (a) in the same direction and (b) in the opposite directions.

is effective in reducing the parasitic coupling and optimizing the filter.

To enhance the magnetic coupling, we modify the width of the spiral tracks. As shown in Figure 4(a), we divide the two coupled resonators into four regions (A, B, C, and D) based on the current directions in the vertical tracks. The magnetic coupling is mainly generated by the currents in regions B and C, which is defined as M_{BC}. The magnetic coupling M_{AC} between regions A and C is weaker than M_{BC}. Due to the opposite current directions in A and B, M_{AC} and M_{BC} have opposite polarities. Similarly the polarity of M_{BD} is opposite to that of M_{BC}. The total magnetic coupling M_M can be written as $M_M=M_{BC}-M_{AC}-M_{BD}$ (M_{AD} is negligible due to large separation). The narrow track carries a larger current density than the wide track in the same resonator, and generates stronger magnetic field radiation. Therefore, by narrowing the tracks in B and C and widening those in A and D (Figure 4(b)), M_{BC} can be increased, while M_{AC} and M_{BD} decreased, resulting in a larger M_M.

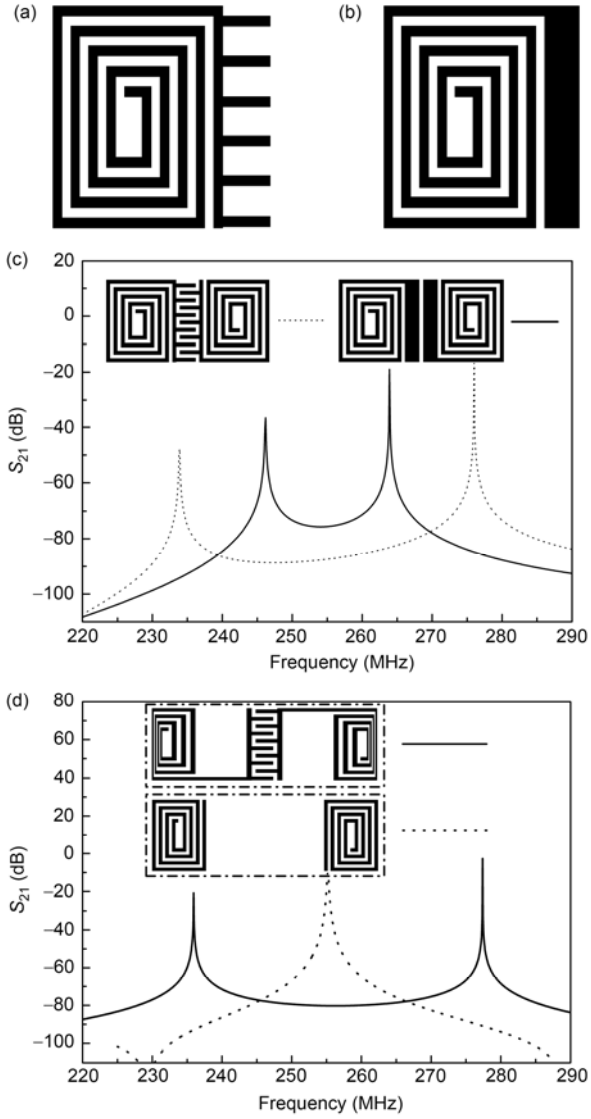

Figure 3 (a) Spiral resonator with parallel finger structure. (b) Spiral resonator with widened outside end. (c) The coupling strength of the two types of resonators from EM simulations. (d) Compared to conventional resonators, parallel fingers generate strong coupling between two resonators with a large separation.

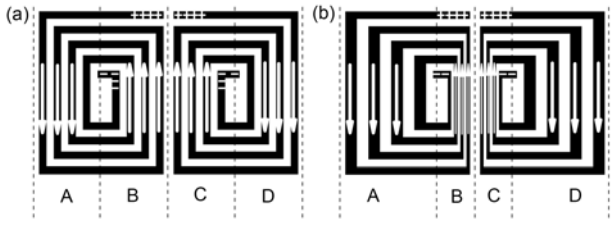

Figure 4 Current directions in coupled resonators. (a) Conventional single-spiral resonators. (b) Spiral resonators with modified track widthes.

Using the methods discussed above, a modified resonator is designed and shown in Figure 5(a). It is well known that the combination of two polarities of coupling is necessary to design a quasi-elliptic function characteristic filter. As is discussed above, the negative coupling can be easily realized between two modified resonators with the same winding direction (such as Figures 5(c) and (d)). The positive coupling only exists between two resonators with opposite winding directions when magnetic coupling is stronger than electric coupling (as shown in Figure 5(b)). We analysed the relationship between the coupling coefficient and the gap for the resonators in Figure 5(b) with different line widths (w) of the tracks near the gap. From Figure 6(a), we see that the narrower the tracks near the gap are, the stronger the positive coupling coefficients are. The positive coupling coefficient can not reach the target value (discussed below) until the tracks are narrowed to 0.06 mm. For the coupled resonators in Figure 5(c) with w=0.06 mm, the coupling coefficient as a function of the gap is shown in Figure 6(b). For the case in Figure 5(d), the coupling coefficient can be tuned over a wide range by changing the length and the number of the parallel fingers. Compared to conventional resonators, the coupling strength for both polarities can be greatly enhanced with these modified resonators, which will be used in our design of filters in VHF band.

2 Filter design and simulations

The filter is designed to meet the following specific re-

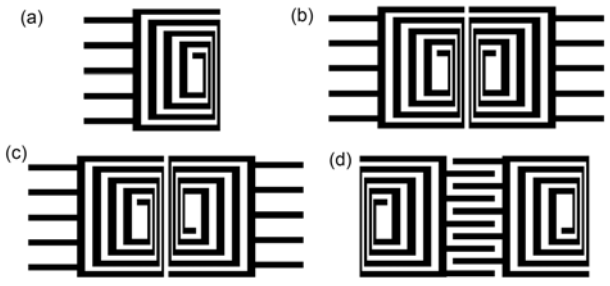

Figure 5 (a) The modified resonator and (b)–(d) three different coupling structures. The coupling coefficients are negative in (c) and (d), and could be positive or negative in (b).

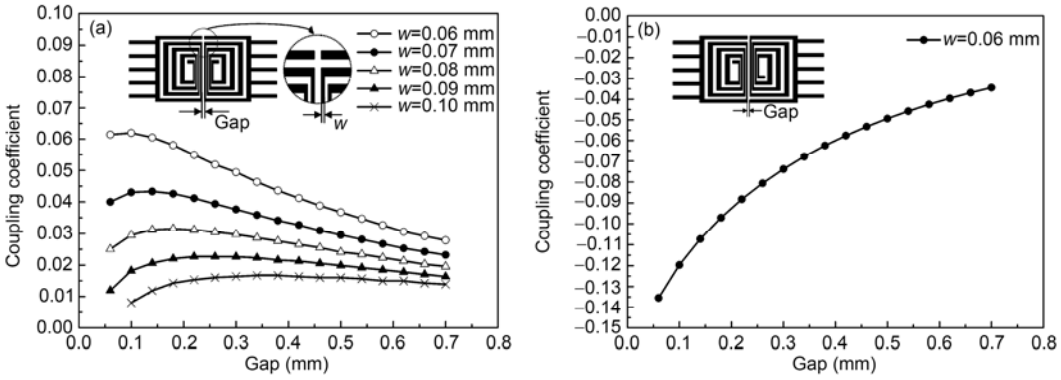

Figure 6 Simulated coupling coefficients as a function of gap between the coupled resonators for (a) the coupled structure in Figure 5(b), and (b) the coupled structure in Figure 5(c). Here *w* represents the linewidth of the tracks near the gap.

quirements:

(i) Center frequency: 255 MHz,

(ii) 3-dB passband bandwidth: 30 MHz,

(iii) Minimum return loss: 15 dB,

(iv) Maximum insertion loss: 0.5 dB,

(v) Out-of-band rejection: >50 dB (<232 MHz and >278 MHz).

To meet the requirements, especially of the out-of-band rejection, we select a ten-pole quasi-elliptic filter. Following the synthesis procedure described in ref. [13], the coupling coefficients of the filter can be calculated:

$$M_{12}=M_{910}=-0.114864,$$
$$M_{23}=M_{89}=-0.071041,$$
$$M_{34}=M_{78}=-0.085318,$$
$$M_{45}=M_{67}=0.05866,$$
$$M_{25}=M_{69}=-0.02208,$$
$$M_{56}=-0.06236,$$
$$Q_1=Q_2=6.30751.$$

Q_1 and Q_2 are external quality factors. The corresponding topology is presented in Figure 7(a). Resonators are aligned into two rows, with solid lines representing the main couplings and the dotted lines representing the cross couplings. Resonators 2–5 or 6–9 with a crossing coupling construct a quadruplet section. Then a cascaded quadruplet (CQ) filter is realized. The CQ filter could provide attenuation poles required by the design of quasi-elliptic filter [14]. In fact, in a quadruplet section, one of the four coupling coefficients should have an opposite sign to the other three to generate attenuation poles at finite frequencies. In our design, we choose M_{45}, the weakest direct coupling, to be positive, while the other three to be negative. As shown in Figure 6(a), the maximal positive coupling coefficient for conventional single-spiral resonators (w=0.1 mm) is 0.0182, far smaller than our target value of 0.05866. On the other hand, the positive coupling coefficient of the modified resonators (w=0.06 mm) with a maximum of 0.062 can reach our target. Therefore it is possible to design a filter that satisfies the required coupling strength using the modified resonators.

Figure 7(b) is the layout of the ten-pole filter using the modified resonators proposed in sect. 1. Resonators 1, 2, 3, and 5 wind clockwise from the center to the outside, while resonator 4 winds anticlockwise. Resonators 2 and 5 are somewhat different from the others. In resonator 2, the tracks at the left and right halves are all narrowed to generate enough coupling with neighboring resonators. The separation between the two halves is also increased by widening the resonator, reducing the parasitic coupling between resonators 1 and 3. In resonator 5, two separate groups of parallel fingers are introduced to generate strong couplings with resonators 2 and 6, respectively. From sect. 1, we know that M_{12}, M_{23}, and M_{25} are negative. M_{34} and M_{45} are couplings between two resonators with opposite winding directions. Electronic coupling dominates in M_{34} because resonators 3 and 4 are separated by a large gap and coupled by parallel fingers; magnetic coupling dominates in M_{45} because of the narrowed tracks. Therefore M_{34} is negative, while M_{45} is positive. The cascaded quadruplet consisting of resonators 2–5 generates two attenuation poles out of the passband. Resonators 6–10 are mirrors symmetrical to resonators 1–5, thus the cascaded quadruplet consisting of resonators 6–9 gives the same attenuation poles as resonators 2–5. We introduce a large separation between the upper half (resonators 1–5) and the lower half (resonators 6–10) to reduce the parasitic coupling. However, the coupling between resonators 5 and 6 is also decreased. Here the parallel fingers between resonators 5 and 6 are used to realize a strong coupling coefficient M_{56}. This is a good example that the parallel fingers can help to reduce the unwanted parasitic coupling without decreasing the direct coupling. We also want to mention that the parallel fingers on resonators 1 and 10 provide an additional way to modify Q_1 and Q_2 which used to be tuned by changing the feedline width and position.

To save the memory and CPU time during the simulation, we set the dielectric loss tangent of $LaAlO_3$ to be zero and the HTS thin film to be lossless. The simulated performance of the filter is shown in Figure 8. From Figure 8 (b), we see the out-of-band transmission response is asymmetric (there

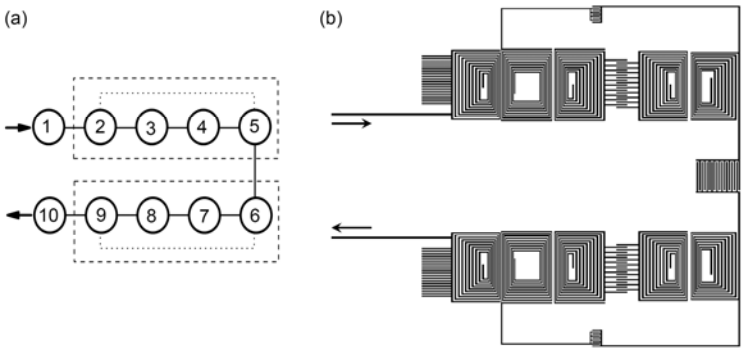

Figure 7 (a) The topology structure (the parts within the dashed line represent quadruplet structures) and (b) the layout of the filter.

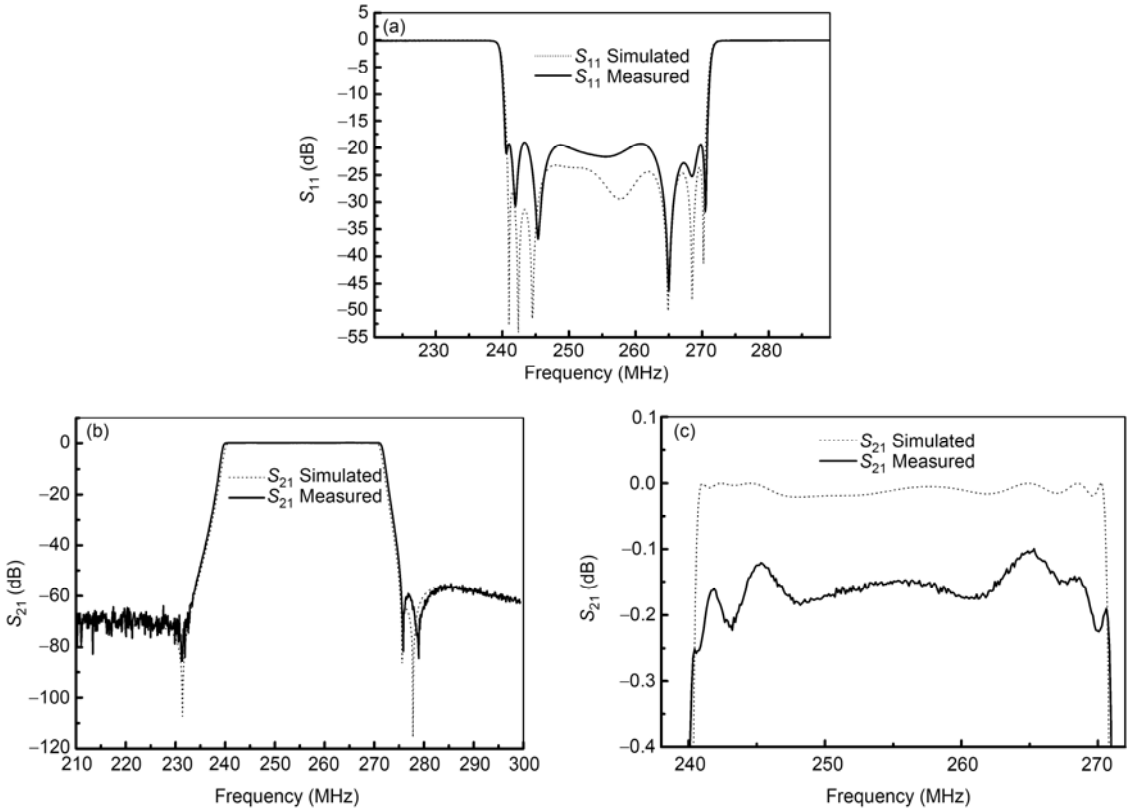

Figure 8 The simulations and measurements of (a) S_{11}, (b) S_{21}, and (c) ripple of the HTS filter.

are two split attenuation poles at the upper stop-band region), because of the residual weak parasitic couplings [15]. To eliminate the parasitic coupling effectively requires a very large separation between the upper half (resonators 1–5) and the lower half (resonators 6–10). Considering that the filter is fabricated on a 2 inch wafer, a moderate separation (8.64 mm) is chosen as a good compromise. From our simulations, the centre frequency is 255.45 MHz, 3-dB bandwidth is 31.5 MHz, the minimum return loss is 23.2 dB, and out-of-band rejection is better than 56.9 dB at the required frequency region.

3 Fabrication and experimental results

The filter was fabricated on a 38.02 mm×36.8 mm×0.5 mm double-sided YBCO film deposited on the $LaAlO_3$ substrate. The standard photolithography and ion-beam milling technology were used for the filter patterning. The wafer was packaged in a shield brass box, which is plated with gold. Some tuning screws were placed on the cover of the box. These tuning screws, which are approximately 1–4 mm high above the HTS circuit, can be used to tune the filter response through modifying the electromagnetic field above the circuit. Due to the errors introduced during the fabrication process, the measured results of the as-prepared filters are usually worse than the simulations. However, by finely tuning the screws the errors can be largely compensated, and the filters recover excellent performance as expected from simulations. The filter enclosed in a cryogenic cooler was measured with a vector network analyzer (Agilent N5230C) at 73 K. A traditional OSLT (Open, Short, Load,

and Through) calibration was performed at room temperature before measurement. The measured result after tuning is shown in Figure 8, and compared with the simulated curves. The measured centre frequency is 255.8 MHz (0.3% larger than the requirement), 3-dB bandwidth and fractional bandwidth are 31.5 MHz (5% wider) and 12.3%, respectively, the maximum insertion loss is about 0.265 dB (a correction of temperature effect on the cables has been considered), the minimum return loss is 17.5 dB, and out-of-band rejection is better than 57.2 dB at the required frequency region. The experimental results show excellent agreement with simulations and basically meet the specification.

4 Conclusion

We designed and measured a 10 pole quasi-elliptic HTS filter with a relatively wide passband (12.3%) in VHF band for radio astronomy application. We modified the single-spiral resonator to enhance the coupling strength and analyzed the coupling polarity. The modified single-spiral resonators can not only enhance the direct coupling, but also reduce the unwanted parasitic coupling. Analysis of the coupling polarity is helpful to design cascaded quadruplet structure that provides attenuation poles to realize quasi-elliptic response.

This work was supported by the External Cooperation Program of the Chinese Academy of Sciences (Grant No. GJHZ1007) and the Knowledge Innovation Program of the Chinese Academy of Sciences (Grant No. KJCX2-YW-W16).

1 Zhang G Y, Huang F, Lancaster M J. Superconducting spiral filters with quasi-elliptic characteristic for radio astronomy. IEEE Trans Microw Theory Tech, 2005, 53: 947–951
2 Yu T, Li C G, Li F, et al. A wideband superconducting filter using strong coupling resonators for radio astronomy observatory. IEEE Trans Microw Theory Tech, 2009, 57: 1783–1789
3 Zhou J, Lancaster M J, Huang F. Superconducting microstrip filters using compact resonators with double-spiral inductors and interdigital capacitors. In: 2003 IEEE MTT-S International Microwave Symposium Digest, Vols. 1–3. Philadelphia: IEEE, 2003. 1889–1892
4 Zhang T L, Yang K, Ning J S, et al. Development of miniature HTSC wide-band filter with open-loop resonators. Chin Sci Bull, 2008, 53: 1300–1303
5 Cui B, Zhang X Q, Sun L, et al. A high-performance narrowband high temperature superconducting filter. Chin Sci Bull, 2010, 55: 1367–1371
6 Wei B, Guo X B, Piao Y L, et al. Field test of HTS receivers on CDMA demonstration cluster in China. Chin Sci Bull, 2009, 54: 612–615
7 Xia H H, Zhou C X, Zuo T, et al. Development of high-temperature superconducting filters operating at temperatures above 90 K. Chin Sci Bull, 2009, 54: 3596–3599
8 Yu T, Li C G, Li F, et al. A novel quasi-elliptic HTS filter with group-delay equalization using compact quasi-lumped element resonators in VHF band. IEEE Trans Appl Supercond, 2009, 19: 69–75
9 Huang F, Zhou M, Yue L B. A narrowband superconducting filter using spirals with a reversal in winding direction. IEEE Trans Microw Theory Tech, 2006, 54: 3954–3959
10 Zhou J, Lancaster M J, Huang F, et al. HTS narrow band filters at UHF band for radio astronomy applications. IEEE Trans Appl Supercond, 2005, 15: 1004–1007
11 Ma Z, Kawaguchi T, Kobayashi Y. Miniaturized high-temperature superconductor bandpass filters using microstrip S-type spiral resonators. IEICE Trans Electron, 2005, E88C(1): 57–61
12 Sonnet Software Inc. EM User's Manual Version 9.0, 2001
13 Hong J S, Lancaster M J. Microstrip Filters for RF/Microwave Application. New York: John Wiley & Sons Inc, 2001
14 Hong J S, Lancaster M J. Design of highly selective microstrip bandpass filters with a single pair of attenuation poles at finite frequencies. IEEE Trans Microw Theory Tech, 2000, 48: 1098–1107
15 Li C G, Zhang Q, Meng Q D, et al. A high-performance ultra-narrow bandpass HTS filter and its application in a wind-profiler radar system. Supercond Sci Technol, 2006, 19: S398–S402